Article

Discovery Medicine 2023; 35(178): 897–909
https://doi.org/10.24976/Discov.Med.202335178.85

Application of Dual-Source CT Using Iterative Reconstruction Technology Combined with CT-FFR Parameters in the Diagnosis of Coronary Heart Disease

Cuicui Wu[1,2], Ziyue Wang[1], Hongxiu Shi[3], Yan Ding[4], Jian Zhou[5], Wenfu Yan[6], Li Wang[5,*]

[1]School of Medical Technology, Qiqihar Medical University, 161000 Qiqihar, Heilongjiang, China
[2]Department of Radiology, Children's Hospital, Zhejiang University School of Medicine, National Clinical Research Center for Child Health, 310051 Hangzhou, Zhejiang, China
[3]The First People's Hospital of Longjiang County, 161000 Qiqihar, Heilongjiang, China
[4]Department of Ultrasound, The Third Affiliated Hospital of Qiqihar Medical University, 161000 Qiqihar, Heilongjiang, China
[5]Medical Imaging Teaching and Research Section, The Third Affiliated Hospital of Qiqihar Medical University, 161000 Qiqihar, Heilongjiang, China
[6]Radiology Department, The First People's Hospital of Longjiang County, 161000 Qiqihar, Heilongjiang, China
*Correspondence: lily1980@qmu.edu.cn (Li Wang)
Published: 1 October 2023

Background and Objective: In order to achieve early detection of myocardial ischemia and improve the diagnosis of coronary heart disease (CHD), it is necessary to find a convenient, non-invasive and effective examination method. This study aimed to explore the application value of dual-source computed tomography (CT) by using advanced modeled iterative reconstruction (ADMIRE) combined with computed tomography-fractional flow reserve (CT-FFR) technique in CHD, which provides imaging basis for early diagnosis of CHD and myocardial ischemia.

Methods: Seventy-five CHD patients were examined by coronary computed tomography angiography (CCTA). Their CCTA images were reconstructed by iterative algorithm in ADMIRE 1–5 using post-processing workstation. The standard deviation (SD), signal-to-noise ratio (SNR) and contrast-to-noise ratio (CNR) of proximal vascular images in right coronary artery (RCA), left main coronary artery (LM), left anterior descending artery (LAD) and left circumflex artery (LCX) were analyzed and compared. Invasive coronary angiography (ICA) was adopted in patients with $\geq$50% stenosis of coronary artery diameter. Taking ICA as the gold-standard method to accurately assess coronary arterial stenosis degree, the diagnostic efficiency of dual-source CT to diagnose coronary artery stenosis was analyzed. Some patients were subjected to myocardial CT perfusion (CTP) scanning and CT-FFR analysis, which facilitated analyzing the correlation and consistency between the diagnostic results of CTP and analysis results of CT-FFR.

Results: There was no statistical difference in the CT values of RCA, LM, LAD and LCX in groups with different ADMIRE reconstruction intensities ($p > 0.05$). But the noise, SNR and CNR interval were different among the iterative intensity groups ($p < 0.05$). Kappa consistency analysis was used to analyze the subjective evaluation results of image quality under different iterative reconstruction grades. The independent sample *t*-test performed on the subjective scores revealed that the scores on images were the best at ADMIRE 4. CCTA has sensitivity, specificity, positive predictive value, and negative predictive value of 91.52%, 97.59%, 97.98%, and 96.42% for identifying coronary artery stenosis, respectively. The diagnostic efficacy of CT-FFR, the Kappa analysis of myocardial CTP and CT-FFR results, which yields a Kappa value of 0.830 ($p < 0.05$). Spearman correlation analysis was used to statistically analyze the results of myocardial CTP and CT-FFR (correlation coefficient r = 0.774, $p < 0.05$). Diagnostic sensitivity and specificity were 93% and 95%, respectively.

Conclusions: The dual-source CT using ADMIRE iterative algorithm has the best display of coronary vessels and higher image quality when the intensity is 4, and CT-FFR can be used as a non-invasive method for early detection of myocardial ischemia, which is worthy of clinical application.

Keywords: dual-source CT; ADMIRE algorithm; non-invasive fractional flow reserve; coronary heart disease

Copyright: © 2023 The Author(s). Published by Discovery Medicine. This is an open access article under the CC BY 4.0 license.
Note: *Discovery Medicine* stays neutral with regard to jurisdictional claims in published maps and institutional affiliations.

Introduction

Dual-source computed tomography (CT) using image reconstruction algorithm is mainly based on iterative algorithms [1]. The general image reconstruction methods mainly include filtered back projection (FBP) and iterative reconstruction (IR) algorithm [2]. As an analytical algorithm, FBP has obvious image noise and unclear details when scanning at low doses [3]. Advanced modeled iterative reconstruction (ADMIRE) is the third generation of reconstruction algorithm in dual-source CT and an algorithm based on the original data domain, image domain and model domain, also known as the three-domain iterative algorithm. On the basis of FBP, a large number of original data are used to reconstruct high-quality images in an iterative manner, providing better technical support for the diagnosis of diseases [4,5]. Different from FBP algorithm, the iterative algorithm can reconstruct a complete image when some original data are missing [6]. After a cyclic iterative process, the artifacts are eliminated to a certain extent and the noise is reduced to obtain high-quality image [7], and image noise is one of the important factors affecting the overall quality of CT image. Reducing image noise and improving image signal-to-noise ratio (SNR) are the goals pursued in the process of updating and iterating medical imaging equipment [8–10]. Computed tomography–fractional flow reserve (CT-FFR) has attained rapid development in recent years, but since it relies on accurate coronary artery and myocardial segmentation for image-based modeling, obtaining high-quality coronary image remains the main goal during coronary computed tomography angiography (CCTA) scanning [11].

Coronary heart disease (CHD), a vascular disease caused by decreased myocardial blood supply due to coronary artery stenosis and clinical symptoms related to myocardial hypoxia [12], is the main cause of death caused by disease worldwide, so accurate assessment of the severity of coronary artery disease is crucial for determining disease treatment strategies [13]. As a non-invasive examination method for screening coronary heart disease [14], CCTA possesses high-density resolution and provides accurate evaluation of coronary narrow degree and analysis of coronary plaque nature [15,16]. CCTA is only used to evaluate the morphology of coronary vessels at the anatomical level [17], and is difficult to determine whether vascular lesions will lead to functional myocardial ischemia by CCTA examination [18]. The non-invasive FFR based on CCTA (CT-FFR) has great advantages in the diagnosis of functional myocardial ischemia.

CT-FFR is an examination technique combining the principles of vascular anatomy and hemodynamics. High-quality CCTA image could provide better diagnostic basis for examining human anatomy [19,20]. CT-FFR achieves the complementary advantages by combining CCTA imaging technology with FFR analysis, and evaluates myocardial ischemia at the anatomical and hemodynamic levels [21]. Dual-source CT using CCTA has high temporal resolution and spatial resolution, and the application of ADMIRE reconstruction algorithm in the third generation allows for the visualization of anatomical morphology of coronary artery [22]. On the basis of CCTA, CT-FFR analyzes the velocity of coronary blood flow and the measurement of the terminal pressure in coronary microcirculation, and then evaluates the coronary blood flow and vascular function; therefore, their combination can improve the clinical decision-making [23].

Materials and Methods

Study Subjects

One hundred patients with clinically suspected CHD were selected for CCTA examination by using dual-source CT (Siemens, SOMAOTM Drive, 472372, Munich, Germany) from May 2021 to October 2021, according to the inclusion criteria and exclusion criteria set forth in the following. It was in line with the Declaration of Helsinki in the World Medical Association (WMA) [24] and has been approved by the Medical Ethics Committee of the Third Affiliated Hospital of Qiqihar Medical College, with the number [2021] No. 101. After excluding 5 cases with respiratory artifacts, 3 cases with poor venous access and 17 cases with myocardial bridge, 75 patients were included in this study. The inclusion criteria of this study are as follows: (1) patients aged 18–80 years old; (2) patients with suspected or diagnosed CHD; and (3) patients without any history of iodine allergy and severe dysfunction in heart, kidney or lung. The exclusion criteria of this study are as follows: (1) patients who could not go through the study due to maniac emotion; (2) patients with severe arrhythmia; (3) pregnant patients; (4) patients with heart failure; and (5) patients with myocardial bridge. The included cases, with an age range of 45–75 years old, had an average age of 61.3 ± 8.8 years old. Subsequently, 25 patients with $\geq$50% stenosis of coronary artery were examined by digital subtraction angiography (DSA), and 2 patients with a history of stent implantation were excluded. Finally, 23 patients were indicated for myocardial CT perfusion (CTP) and CT-FFR analysis.

Scanning Methods and Image Post-Processing

CCTA Data and Post-Processing

The patients were scanned, while lying in a supine position, by CCTA combined with dual-source spiral CT (Siemens Somatom Drive, 463162, Siemens AG, Munich, Germany), with scanning range covering the bifurcation of trachea to 1–2 cm below diaphragm. The width of the detector was 128×0.6 mm, and the layer thickness was 0.75 mm. The scanning parameters included tube voltage (100 kV); tube current, which was automatically adjusted by Care Dose 4D (reference of tube current as 200–300 mAs); and pitch, which was automatically adjusted. For patients with heart rate $<$70 bpm, the window of reconstruc-

Table 1. Subjective criteria for scoring image quality.

Grades	Evaluation criterion
1	Blurred image showing unclear blood vessels and unidentified lumen structure could not aid in definite diagnosis by physicians
2	Image with obvious artifacts, multiple interruptions of blood vessels and obvious faults affected diagnosis results
3	Image with poor image display, blurred vascular edge or split layer did not affect the overall diagnosis
4	Image that met diagnostic criteria with slightly unclear local blood vessels could aid in definite diagnosis
5	Image with clear display, complete lumen and sharp vessel wall could aid in definite diagnosis

tion time was at mid relaxation period (about 70%–75% of R-R interval). For patients with heart rate in 70–80 bpm, the window of reconstruction time in right coronary artery (RCA) was systolic end (35%–45% of R-R interval), and the best window of reconstruction time in the left coronary artery (LCA) was diastolic middle (about 70%–75% of R-R interval). In addition, for patients with heart rate >80 bpm, the window of reconstruction time was systolic end (35%–45% of R-R interval). The optimal phase of displaying coronary artery was selected based on the patients' heart rate for data reconstruction.

Empower CTA+ (Imaxon Pty Ltd, 246154, Toronto, Canada) double-barrel high-pressure syringe was used for the injection of contrast agent. The right median cubital vein was punctured with an intravenous detaining needle (20 G), and 10 mL of normal saline was injected in advance to check whether the venous access was normal. The total amount of injection was about 50–70 mL obtained by the calculation of 1–1.2 mL/kg, and the injection rate was 5.0 mL/s. The scan was started 5 s after the injection of contrast agent iopamidol (370 mgI/mL; Beilu, Beijing, China). Retrospective electrocardiogram (ECG)-gated scanning and contrast agent tracking were used in this study for scanning, and the region of interest was fixated at the aortic root of pulmonary artery trunk, taking 100 HU as trigger threshold. The scan was automatically triggered, and then 50 mL of normal saline was injected at a rate of 5.0 mL/s when the CT value of intravascular contrast agent concentration in the region of interest reaching preliminary threshold.

After completing CCTA scanning, all data were transmitted to post-processing workstation (Syngo Acquisition Workplace), and the images of each patient were reconstructed using ADMIRE in grades 1–5, with convolution kernel set as 126f medium smooth light sensibility ordinance (LSO), reconstruction thickness at 0.75 mm and reconstruction increment at 0.5 mm. The curved planar reconstruction (CPR), multiple planar reconstruction (MPR), maximum intensity projection (MIP) and volume reformation (VR) were performed on RCA, left main coronary artery (LM), left anterior descending artery (LAD) and left circumflex artery (LCX) of each patient to assess initial position, walking, stenosis degree of coronary artery and the position between plaque and lumen in multiple directions.

Invasive Coronary Angiography Data and Post-Processing

Coronary angiography was performed using dual-plate DSA (Philips, UNIQ20, Amsterdam, Netherlands). Before angiography, consent was obtained from the patients after they had been informed of the adverse reactions of contrast agent. Patients lying in supine position were routinely monitored with ECG before examination and disinfected before angiography. The local infiltration anesthesia was performed with 2% of lidocaine. Conventionally, radial or femoral arteries of patients were punctured via the modified Seldinger method, and corresponding multifunctional catheters were inserted to left and right coronary arteries, followed by iodixanol injection (320 mgI/mL) and coronary angiography. The lesions of left and right coronary artery trunk and its branches were observed and assessed by the conventional six-position method and three-position method in multi-angle projection. Meanwhile, patients' condition, ECG monitoring and pressure curve were closely observed.

Acquisition Method of Myocardial CTP Data

The ultra-high 256-row Revolution APEX CT (GE company, 3300422, Boston, MA, USA) was used. The basic scanning parameters included 80 kV of tube voltage, 200 mAs of tube current, and 60% adaptive statistical iterative reconstructions-V (ASiR-V) in multi-model IR. A prospective scanning protocol, taking into account the calcification score in cardiac coronary artery at a low dose, was used to scan from 1–2 cm below tracheal bifurcation to cardiac apex, so as to obtain plain scan images of the heart. The contrast agent was injected at a rate of 5 mL/s using a double-barrel syringe. A non-ionic iodine-containing contrast agent, called ioversol, was used at a dose of 370 mg/mL and a volume of 50 mL. An injection of 30 mL of 0.9% sodium chloride was administered at the same rate to trigger myocardial perfusion scanning during systole. Data on myocardial perfusion at rest were collected. Due to the risk of stress myocardial perfusion scan, myocardial perfusion at rest was prioritized and used instead. Myocardial blood flow (MBF) value in normal myocardial perfusion was 104.8–142.9 mL/100 mL/min, and MBF value in low myocardial perfusion was 52.0–96.0 mL/100 mL/min. MBF <75 mL/100 mL/min indicated high-risk blood perfusion area, and MBF <96 mL/100 mL/min showed the basis for the diagnosis of myocardial ischemia.

CT-FFR Data and Post-Processing

CT-FFR measurement was implemented by CT-FFR (DEEPVESSEL FFR, Keya Medical, Beijing, China) based on deep learning to evaluate and measure the physiological function of coronary artery. Patients with 30%–90% of coronary artery stenosis were selected. The high-quality CCTA images displaying coronary artery were transmitted to the Keya non-invasive FFR backstage in digital imaging and communications in medicine (DICOM) format, and CT-FFR analysis was performed by relevant technicians at the backend. The medical image information of coronary artery in DICOM format was reconstructed by structural analysis module, and then FFR value was calculated by the functional analysis module. Deep learning, medical images and physiological function were adopted to evaluate heart function, and finally CT-FFR results were obtained to quickly evaluate whether coronary stenosis leads to functional myocardial ischemia and to provide anatomical and functional information, which are instrumental to clinical decision-making.

Image Quality Assessment

Objective and Subjective Evaluation of CCTA and DSA

The results of CCTA were scored by two chief physicians in imaging department through double-blind method. When there were controversies in the diagnosis results, the third chief physician was approached to adjudicate the conflict until a unanimous result was reached. The final diagnostic results of DSA, in the form of coronary angiography images, were evaluated by two experienced cardiologists through a double-blind method. When the diagnostic results of the two physicians were different, a discussion would be initiated until a final decision was reached. The image quality of RCA, LM, LAD and LCX, which were divided into 15 segments according to the American Heart Association (AHA), was evaluated [25]. The image quality of coronary artery was graded using 5-point Likert scoring method (Table 1).

Table 2. General data of patients.

Parameters	Numbers
N (cases)	75
Gender (male/female)	44/31
Age (year)	61.3 ± 8.8
DLP (mGy × cm)	712.7 ± 281.1
ED (mSv)	9.9 ± 3.9

Notes: DLP, total radiation dose; ED, effective radiation dose.

Diameter method [26] is commonly used to measure coronary artery stenosis. Images showing the most severe coronary artery stenosis examined by CPR were selected. The diameter of proximal normal lumen (a) on the image was measured, and the diameter of lumen affected by the worst stenosis (b) was visually measured. The formula of the degree for coronary artery stenosis is given below:

Degree of coronary artery stenosis = (a – b)/a

The objective values of all data were measured in post-processing workstation (Syngo Acquisition Workplace), and the regions of interest were set in the proximal vascular area of RCA, LM, LAD and LCX. The CT and noise values were measured at the four positions. The noise value is the standard deviation (SD) of the image; the SNR is given by dividing the CT value of region of interest by noise value; and the contrast-to-noise ratio (CNR) is represented by the difference between the CT value of region of interest and the CT value of adjacent fat/noise value of region of interest.

Evaluation of CT-FFR Data

Clinically, taking 0.80 as the threshold, CT-FFR value $\leq$0.80 suggested the presence of myocardial ischemia, and CT-FFR value $>$0.80 suggested small possibility of myocardial ischemia caused by the lesion, which requires no clinical intervention. In this study, we also took the threshold (0.80) as the basis for assessing myocardial ischemia. Generally, CT-FFR value range of 0.75–0.80 was considered a range of borderline values. Whether interventional therapy was needed as a treatment should be based on the results of other related examinations and clinical manifestations.

Statistical Analysis

All experimental data were processed using Microsoft Excel (Version: 2019, Microsoft Corporation, Redmond, WA, USA), and statistical analysis was performed using SPSS 22.0 software (Version: 22.0, International Business Machines Corporation, Armonk, NY, USA). The normality of data was tested, and the data are expressed as mean $\pm$ standard deviation. The homogeneity of variances of quantitative data was assessed, and the CT values of the objective evaluation indexes in ADMIRE reconstruction intensity images at all grades were compared by one-way analysis of variance (ANOVA). Noise, SNR and CNR were analyzed by Tamhane's T2 test. Paired sample *t*-test was used to analyze the difference between the scores obtained from two physicians. Independent sample *t*-test was performed on the subjective scores of CCTA image quality in F1–F5, which are the patient groups divided based on different iterative reconstruction grades. Kappa consistency test was used to test the consistency between diagnosis results of invasive coronary angiography (ICA) and CCTA, and myocardial CTP and CT-FFR. Pearson's correlation analysis was used to analyze the correlation. McNemar test of paired χ^2 test was used to test whether there was a difference between the two methods.

Results

General Data

A total of 100 patients with clinically suspected coronary atherosclerotic heart disease were selected. After excluding 5 cases with respiratory artifacts, 3 cases with poor venous access, and 17 cases with myocardial bridge, 75 patients were included in this study. There were 44 males and 31 females, who had an average age of 61.3 $\pm$ 8.8 years (Table 2). According to different iterative reconstruction grades, they were divided into five groups, namely ADMIRE 1 through ADMIRE 5.

Regarding the grouping principle of coronary CT image quality, the intensity of dual-source ADMIRE iterative reconstruction was divided into 5 intensities, and thus, all the reconstructed data were divided into 5 groups according to the different intensity levels of iterative reconstruction. The analysis and comparison between the iterative intensity groups were carried out.

Objective Assessment of CCTA Image Quality

CT values under different iterative reconstruction grades met the homogeneity of variances. There was no statistical difference in CT values of groups with different ADMIRE reconstruction intensity in RCA, LM, LAD and LCX using one-way analysis of variance (ANOVA) ($p > 0.05$). Tamhane's T2 test showed that the noise, SNR and CNR of proximal RCA, LM, proximal LAD and proximal LCX were significantly different between the groups with interval iterative strength ($p < 0.05$). Table 3 showed a table on mean value analysis of objective evaluation indexes in coronary vascular branches, and it can be seen intuitively in Fig. 1. With increased ADMIRE intensity, the image noise gradually decreased, and SNR and CNR gradually increased. As shown in Fig. 2a–e revealed more delicate image with the increase of iterative reconstruction intensity. Fig. 2f showed the calcification distribution of coronary vascular tree.

Subjective Evaluation of CCTA Image Quality

In order to compare the subjective scores under different iterative reconstruction grades, a one sample *t*-test was used. The quantitative data were expressed as mean $\pm$ standard deviation. The highest grade of coronary artery images under different iterative reconstruction grades evaluated by two physicians was grade 4 of ADMIRE (4.64 $\pm$ 0.64/4.62 $\pm$ 0.65, respectively), as shown in Table 4. In order to achieve more accurate comparison between the scores of the two radiologists, the paired sample *t*-test was adopted. After statistical analysis, it was found that *p* values of the two subjective scores were far greater than 0.05, so there was no difference between the two scores. Considering that the display effect of different plaque properties under different iterative reconstruction grades was slightly different, the image quality of ADMIRE in grade 4 was recommended for the diagnosis of coronary artery stenosis in this study.

Diagnostic Efficacy of Dual-Source CT for Coronary Artery Stenosis

The diagnostic efficacy of dual-source CT was evaluated, and the diagnostic efficacy of CCTA was calculated with ICA as the reference. A total of 308 coronary vascular segments were available for diagnosis. The consistency analysis of ICA and CCTA showed that Kappa value was 0.845 ($p < 0.05$), which was statistically significant. Table 5 shows that the sensitivity, specificity, positive predictive value and negative predictive value of dual-source CT angiography in the diagnosis of coronary artery stenosis were 91.52% (54/59), 97.59% (243/249), 90% (54/60) and 97.98% (243/248), respectively, and the diagnostic consistency rate was 96.42% (297/308).

Diagnostic Efficacy of CT-FFR for Myocardial Ischemia

The diagnostic efficacy of CT-FFR for myocardial ischemia was evaluated. Taking myocardial CTP as the reference, the consistency between diagnosis results of myocardial CTP and CT-FFR results was analyzed using Kappa analysis, which yielded a Kappa value of 0.830 ($p < 0.05$). Pearson's correlation analysis was used to statistically analyze the results of myocardial CTP and CT-FFR, showing a correlation coefficient, r = 0.774 ($p < 0.05$) (Fig. 3). In clinical practice, FFR $\leq$0.80 was mostly used as the threshold for the diagnosis of vascular stenosis; the detection results of CT-FFR $\leq$0.80 suggested myocardial ischemia, whose diagnostic sensitivity and specificity were 93% (13/14) and 95% (52/55), as detailed in Table 6.

Fig. 4 shows the CPR image of each branch of the coronary artery and the comparison of CT-FFR results, and the lumen stenosis caused by multiple plaques in the right coronary artery. The corresponding CT-FFR value of RCA is 0.77, which implies that the myocardial area supplied by the RCA may have insufficient blood supply. However, there are multiple calcifications and mixed plaque shadows at the opening and the middle section of LAD, and the CT-FFR value of the corresponding LAD is 0.79, indicating that the area supplied by the severely narrowed blood vessels does not cause serious myocardial ischemia. Therefore, CT-FFR results can be interpreted along with CCTA examination results and clinical manifestations in making the diagnosis and treatment decision for patients so as to avoid unnecessary percutaneous coronary intervention (PCI) treatment.

Discussion

Improved Coronary Image Quality by Iterative Reconstruction Technology of ADMIRE

The application of CT technology improves the accuracy of CCTA [27], which is now widely used as a substitute for ICA in the differential diagnosis of coronary artery disease [28]. The advantage of CCTA is that it can exclude di-

Table 3. Objective evaluation index of coronary vascular branches.

Reconstruction grades	CT value	Noise	SNR	CNR
RCA (n = 75)				
ADMIRE 1	448.9 ± 102.4	37.6 ± 13.5	11.1 ± 5.2	13.4 ± 5.5
ADMIRE 2	450.5 ± 113.3	32.8 ± 13.8	14.1 ± 9.2	16.7 ± 10.2
ADMIRE 3	457.1 ± 108.3	28.0 ± 11.8	16.1 ± 8.1	19.3 ± 9.1
ADMIRE 4	461.2 ± 114.9	23.3 ± 11.2	20.4 ± 11.3	24.3 ± 12.5
ADMIRE 5	472.9 ± 113.1	20.3 ± 10.4	24.6 ± 14.2	29.3 ± 16.4
F	0.528	22.573	19.350	21.172
p	0.715	0.000	0.000	0.000
LM (n = 75)				
ADMIRE 1	460.7 ± 95.8	25.1 ± 8.2	18.1 ± 13.4	20.2 ± 7.7
ADMIRE 2	461.9 ± 96.0	21.6 ± 7.6	19.7 ± 8.2	23.8 ± 9.4
ADMIRE 3	463.1 ± 95.7	20.3 ± 5.2	22.7 ± 9.9	27.5 ± 11.2
ADMIRE 4	468.7 ± 98.9	16.2 ± 16.2	27.1 ± 11.7	32.9 ± 13.2
ADMIRE 5	472.2 ± 99.9	14.1 ± 5.9	31.5 ± 13.1	38.2 ± 15.0
F	0.177	15.457	16.048	26.532
p	0.950	0.000	0.000	0.000
LAD (n = 75)				
ADMIRE 1	440.6 ± 81.6	42.7 ± 11.2	12.8 ± 3.6	10.9 ± 3.0
ADMIRE 2	447.1 ± 82.5	37.9 ± 11.7	14.7 ± 4.4	12.6 ± 3.6
ADMIRE 3	450.3 ± 83.3	33.5 ± 11.3	17.0 ± 5.6	14.6 ± 4.6
ADMIRE 4	457.2 ± 85.0	30.3 ± 12.5	20.3 ± 8.1	17.3 ± 6.8
ADMIRE 5	452.3 ± 83.9	27.4 ± 12.9	23.7 ± 10.3	20.2 ± 8.7
F	0.614	11.875	18.589	18.878
p	0.653	0.000	0.000	0.000
LCX (n = 75)				
ADMIRE 1	425.6 ± 97.9	37.3 ± 12.4	12.4 ± 6.4	12.4 ± 4.4
ADMIRE 2	431.6 ± 99.2	31.9 ± 11.3	14.7 ± 7.4	14.8 ± 5.2
ADMIRE 3	433.9 ± 101.0	28.2 ± 10.7	17.2 ± 9.4	1.4 ± 7.0
ADMIRE 4	437.6 ± 101.0	24.1 ± 10.5	21.3 ± 13.5	21.6 ± 10.5
ADMIRE 5	445.8 ± 102.9	20.5 ± 10.0	28.0 ± 21.0	28.3 ± 17.5
F	0.227	14.537	9.594	15.606
p	0.923	0.000	0.000	0.000

Notes: Grades 1–5 in ADMIRE indicated different iterative reconstruction grades. All data presented in this table are expressed as mean ± standard deviation, except for F-value and *p*-value. CT, computed tomography; SNR, signal-to-noise ratio; CNR, contrast-to-noise ratio; RCA, right coronary artery; ADMIRE, advanced modeled iterative reconstruction; LM, left main coronary artery; LAD, left anterior descending artery; LCX, left circumflex artery.

agnosis of several anatomical coronary artery diseases and provide a detailed assessment of atherosclerotic burden and plaque morphology [29,30], enabling efficient diagnosis of coronary artery disease and early application of preventive treatment. The ADMIRE algorithm in dual-source CT is the third generation of iterative algorithm technology, that is, three-domain iterative algorithm, which can better remove artifacts, reduce noise, and improve image quality [31]. ADMIRE is a three-domain iterative technique based on original data domain, image domain and model domain [32]. The correction cycle is introduced in the process of image generation, and this iterative information capitalizes upon original data to improve image quality [33]. Iterative reconstruction, one of the most widely used noise reduction techniques, achieves higher image quality than FBP does by using complex mathematical techniques to construct image noise [34,35]. As a non-invasive examination method of angiography, dual-source CT can clearly show the morphology of coronary vessels through more advanced IR and post-processing methods, making the accurate evaluation of coronary artery lesions at various stages more convenient [36]. IR, dual-source technology and scanning technology for covering the whole heart are widely used to improve the image quality of coronary artery [37].

In this study, dual-source CT using iterative algorithm of ADMIRE was used to improve the quality of coronary artery imaging, so as to facilitate the early detection of coronary artery stenosis and to plan the corresponding intervention treatment of the lesion vessels during early stage. By performing CCTA examination on the heart and itera-

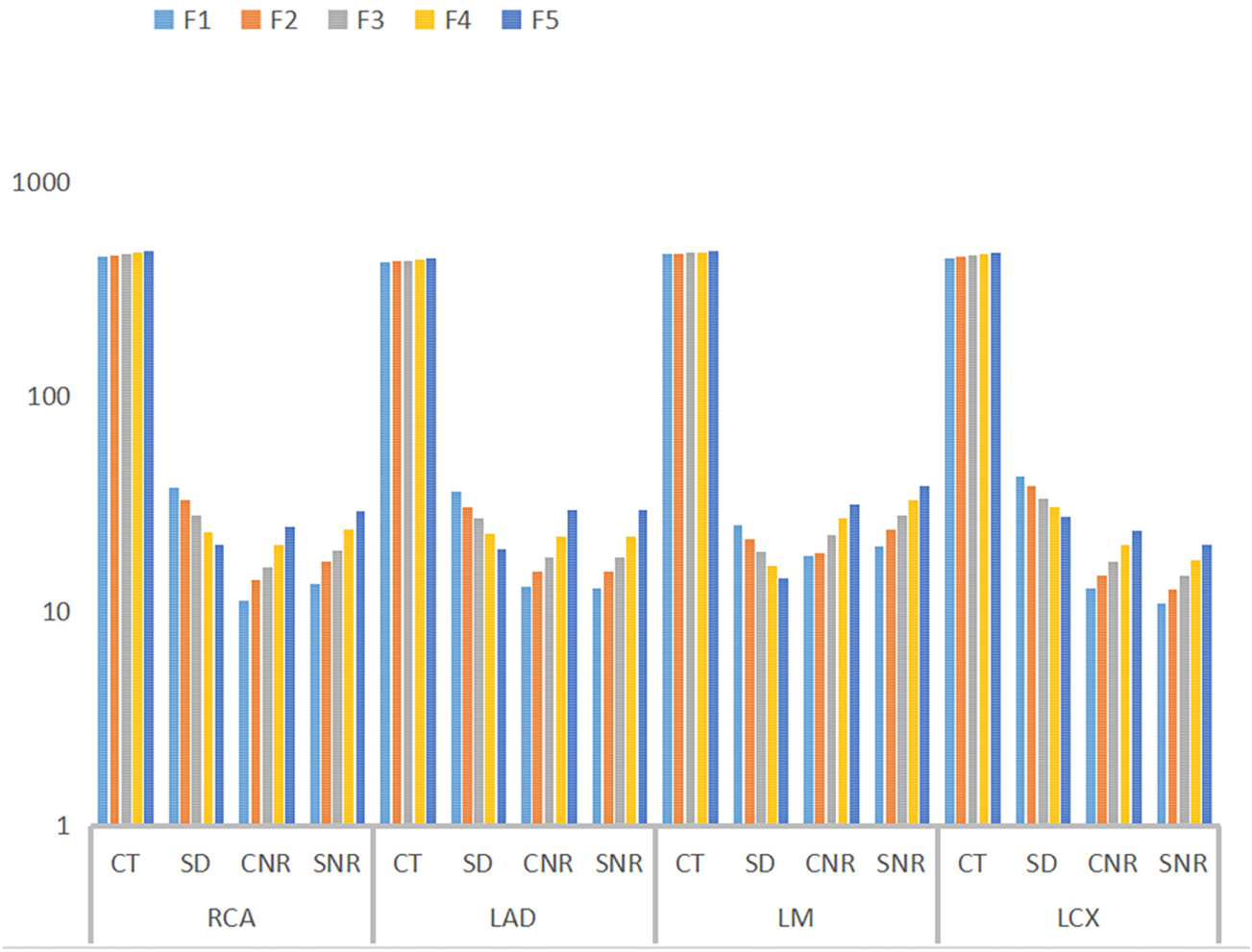

Fig. 1. Relative changes of mean values of each parameter under different reconstruction grades in coronary artery branches. F1–F5 refer to the 5 grades of ADMIRE's iterative reconstruction. SD, standard deviation.

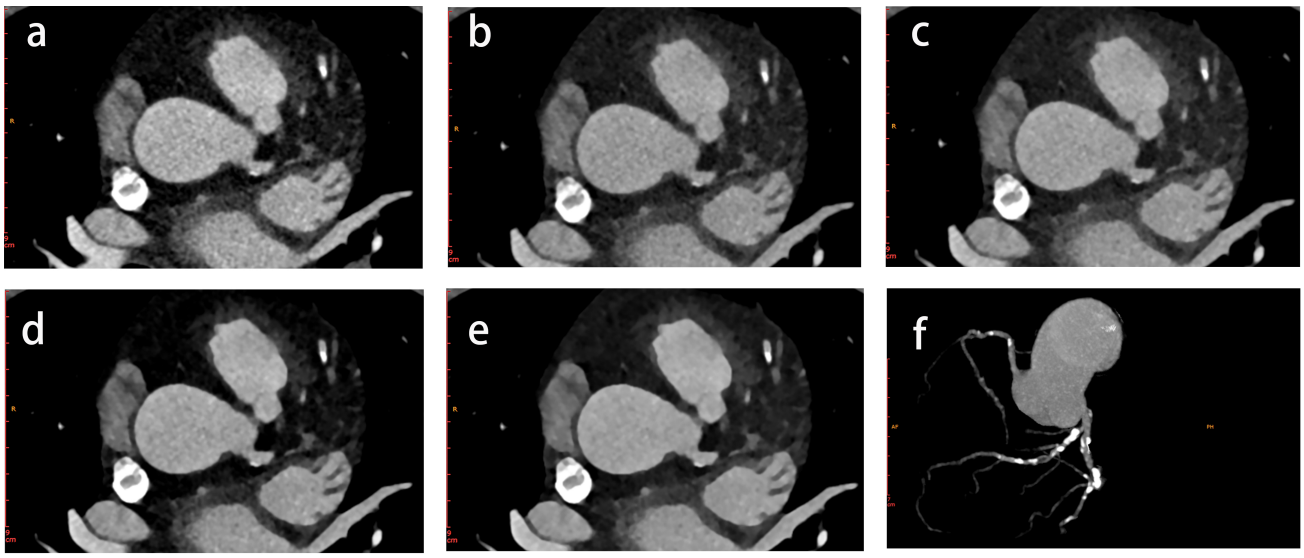

Fig. 2. Images of coronary artery with different iterative reconstruction levels. (a–e) Images under ADMIRE iterative reconstruction in grades 1–5, respectively. (f) Calcification distribution of coronary vascular tree.

Table 4. Analysis of subjective scores by the two physicians (n = 70).

Reconstruction grades	Physician 1	Physician 2	*t*-value	*p*-value
	Scores	Scores		
F1	2.93 ± 0.61	2.95 ± 0.62	0.445	0.658
F2	3.28 ± 0.68	3.31 ± 0.65	0.815	0.418
F3	4.53 ± 0.72	4.54 ± 0.68	0.376	0.708
F4	4.64 ± 0.64	4.62 ± 0.65	0.705	0.483
F5	4.36 ± 0.62	4.37 ± 0.63	0.376	0.708

Notes: The scores are expressed as mean ± standard deviation, and F1–F5 indicate different iterative reconstruction grades.

Table 5. Diagnostic efficacy of CCTA for coronary artery stenosis (vascular level).

ICA	CCTA		Total
	Negative	Positive	
Negative	243	6	249
Positive	5	54	59
Total	248	60	308

ICA, invasive coronary angiography; CCTA, coronary computed tomography angiography.

Table 6. Comparison of CT-FFR results with diagnostic results of myocardial CTP.

CT-FFR	Myocardial perfusion		Total
	Negative	Positive	
Negative	52	3	55
Positive	1	13	14
Total	53	16	69

CT-FFR, computed tomography-fractional flow reserve; CTP, CT perfusion.

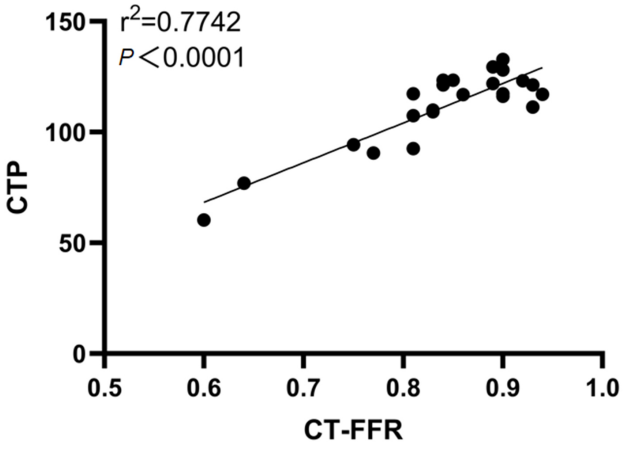

Fig. 3. Pearson correlation analysis of CT-FFR and myocardial CTP.

tive reconstruction of ADMIRE 1–5, we respectively evaluated the main branches of coronary arteries and considered that objective imaging approach and subjective evaluation under different iterative reconstruction grades were the most suitable for displaying coronary plaques and had the highest image quality at 4-level ADMIRE, regardless of the imaging in RCA, LM, LAD or proximal LCX. This is consistent with the research results by Javaid *et al*. [38] We also considered that the ADMIRE reconstruction intensity at grade 4 was the most suitable for CCTA scanning. At present, dual-source CT is widely used in clinical practice, and its application in coronary angiography is becoming more developed. In a study by Xia *et al.* [39], dual-source CT, combined with CCTA, improves the quality of images used in the examination and diagnosis of CHD in the elderly, meeting the requirements of clinical diagnosis. On the other hand, Ellmann *et al.* [40] showed that patients in different body mass index (BMI) groups have the best image presentation effect in ADMIRE at grade 3. In addition, iterative reconstruction technology in ADMIRE has also been studied abroad. Tian *et al.* [41] reported that noise attenuation and iterative reconstruction technology based on deep learning could significantly improve the quality of CCTA image, reduce the image noise by more than 20%, and improve the objective and subjective image quality by about 40% without excessive smoothing. Another study also showed that the application of deep learning and iterative reconstruction technology can improve the noise reduction performance, and significantly improve objective and subjective quality of CCTA images without excessive smoothing [42]. In order to pursue higher-quality images and achieve early detection and treatment of CHD, the optimization of reconstruction algorithm in dual-source CT has become the focus of research.

Non-Invasive FFR

Non-invasive FFR, also known as CT-FFR, is based on CCTA image modeling, and its excellent CCTA image quality has a great influence on the results of CT-FFR analysis [43]. CT-FFR mainly includes CT-FFR based on contrast discrimination function (CDF) and CT-FFR based on deep learning. Since CT-FFR based on contrast discrimination function is only suitable for small-sized, single-type data sets, it is inappropriate to apply it to a large-sized multi-type data sets, as this would lead to difficult application in clinical settings [44,45]. CT-FFR (DEEPVESSEL FFR,

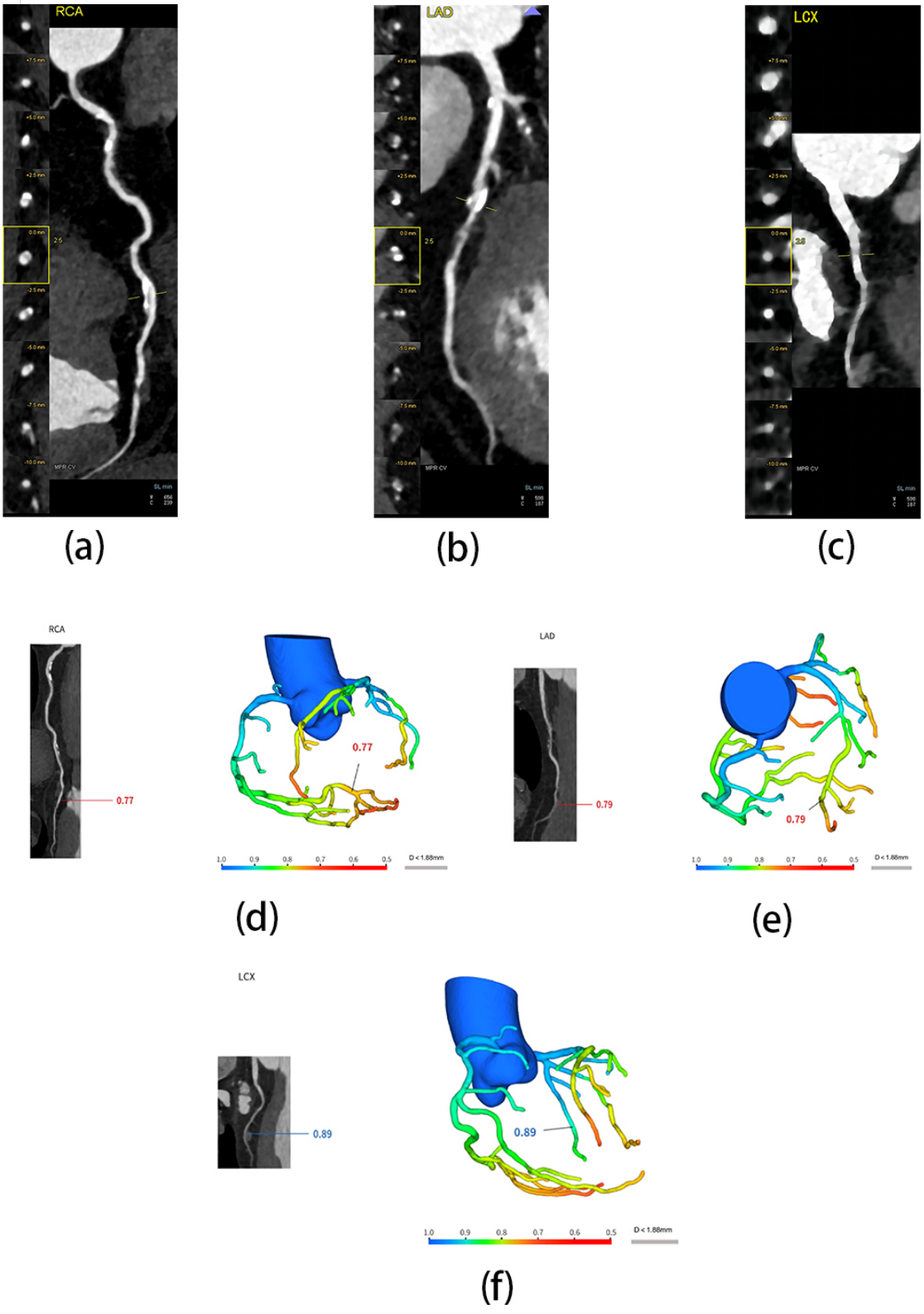

Fig. 4. The CPR of angiostenosis in CCTA on a 62-year-old male, as well as the analysis and comparison of the CT-FFR results. (a–c) Images of CPR of RCA, LAD and LCX. (d–f) CT-FFR values of RCA, LAD and LCX. CPR, curved planar reconstruction.

Keya Medical) based on deep learning used in this study fully combines the advantages of multi-layer neural network and recurrent neural network. The former learns the image features, structural features and functional features of each point on coronary artery, while the latter combines the local feature vectors of each point on blood vessels, considers the whole blood vessel tree as a whole, and obtains accurate blood flow characteristics. These two networks

are functionally complementary to each other and could quickly and accurately predict the FFR value on the blood vessel [46,47]. The model directly trained by relevant models can be to process new measurement data after learning the anatomical structure and blood flow of coronary vessels on the basis of high-quality image data of CCTA and extracting the key feature parameters [48].

Coronary artery disease reporting and data system (CAD-RADS) 2.0 classification follows the framework of stenosis evaluation, plaque burden and correction factor, and selects CT-FFR or myocardial CTP for ischemic assessment [49]. Firstly, the dual-source CT using CCTA has high temporal resolution and spatial resolution, while the dual-source CT using third-generation reconstruction algorithm in ADMIRE clearly displays anatomical morphology of coronary artery [50]. The combination of CCTA and CT-FFR enables a more accurate diagnosis of the nature of the disease and provides suggestions for later treatment [51]. How CT reconstruction algorithm affects CT-FFR analysis has been studied. A foreign study demonstrated analyzing vascular data that had been reconstructed by spatial iterative reconstruction and FBP by CT-FFR in CCTA [52]. After analysis, it was found that the CT-FFR values of each vessel reconstructed by iterative reconstruction in image space (IRIS) and FBP were significantly different, and CT reconstruction algorithm would affect the results of CT-FFR analysis [53]. In addition, iterative reconstruction algorithm also improves the post-processing speed of CT-FFR. CT-FFR can analyze the velocity of coronary blood flow, measure terminal pressure of coronary microcirculation, and evaluate coronary blood flow and vascular function. Therefore, their combination can reduce the false positive results of myocardial ischemia. To a certain extent, it can provide guidance for PCI decision-making and reduce unnecessary overtreatment [54,55]. A trial has shown that early PCI in patients with stable coronary artery disease, who were categorized based on the severity of angiographic stenosis, did not significantly reduce coronary events, compared to those taking early drug therapy [56]. Relying solely on the results of coronary angiography to make the next decision for patients will result in unnecessary PCI treatment and coronary artery bypass grafting (CABG) revascularization [57]. In clinical settings, CCTA and CT-FFR results should be combined while evaluating the patients. After comprehensively assessing the anatomical information of the lesion site provided by CCTA and the myocardial functional information provided by CT-FFR examination, and evaluating the patients' clinical symptoms, the next treatment for patients could be decided to improve the diagnosis rate as much as possible [58,59].

Due to long analysis time, CT-FFR is mainly applied to the patients with stable angina pectoris. Some researchers have evaluated the real clinical utility of CT-FFR based on CCTA in the decision-making of patients with stable coronary artery disease (CAD), and showed that CT-FFR detection is feasible in patients with moderate stenosis diagnosed by CCTA, corroborating that CCTA-based CT-FFR has a certain impact on the subsequent clinical diagnosis and treatment of patients [60]. Delayed ICA in patients with CT-FFR >0.80 has a good short-term prognosis. FFR and myocardial perfusion by positron emission tomography (PET) can be used as the gold standard for evaluating myocardial ischemia. FFR, as the gold standard for evaluating non-invasive CT-FFR [61], is an invasive examination method. Vasodilators are needed while performing these techniques, which also expose the patients to a high dose of radiation [62]. As a powerful tool in facilitating current cardiovascular practice and guiding revascularization decisions, perfusion imaging of PET is technically advanced and widely used in current cardiac imaging [63], but this imaging technique is costly, invasive, and complex in terms of technology. Due to some limitations, perfusion imaging of PET was not considered in this study [64]. However, the studies by Chinnaiyan *et al.* [65], Beg *et al.* [66] and Gajanan *et al.* [67] have shown that non-invasive CT-FFR and invasive FFR complementary to each other, and verified the accuracy and feasibility of CT-FFR. The study by Chen *et al.* [68] has shown that the diagnostic performance of non-invasive CT-FFR based on CT in the diagnosis of coronary artery stenosis was comparable to that of FFR. In this study, myocardial CTP imaging was used as the gold standard for the diagnosis of myocardial ischemia, and the correlation between the diagnostic results of myocardial CTP and CT-FFR results was analyzed.

This study is constrained by some limitations. Firstly, it failed to assess the impact of different iterative reconstruction grades on multifarious natures of plaques. Secondly, due to trauma, invasive FFR examination was not used as the gold standard to evaluate the diagnostic performance of CT-FFR, and results of myocardial CTP, instead of invasive FFR examination, were used. Thirdly, very few cases were included in the CT-FFR analysis in this study.

In summary, CCTA scanning using ADMIRE iterative algorithm can effectively improve the image quality, and the coronary artery can be best displayed especially in ADMIRE reconstruction intensity at grade 4. In addition, non-invasive CT-FFR can be used as an examination method to evaluate myocardial ischemia and provide guidance for PCI decision-making.

Conclusions

In this study, the image data on coronary artery of included cases were used for iterative reconstruction by ADMIRE in grades 1–5. With the increase of iterative reconstruction intensity, the CNR and SNR of CCTA image gradually increased, and when the iterative reconstruction intensity of ADMIRE equal to 4, the quality of CCTA image had a huge positive influence on the diagnosis.

Taking the diagnosis results of invasive DSA in coronary artery as the gold standard, dual-source CT was found to possess high sensitivity, specificity and diagnostic rate

in the diagnosis of CHD, confirming that dual-source CT using iterative reconstruction technology of ADMIRE is of great significance in the diagnosis of coronary artery stenosis.

In this study, the correlation and consistency between the results of myocardial CTP and CT-FFR were statistically significant. Moreover, with high sensitivity and specificity in the diagnosis of vascular stenosis, which can provide a basis for later revascularization and imaging data for clinical decision-making while alleviating the pain of patients.

Availability of Data and Materials

Data to support the findings of this study is available on reasonable request from the corresponding author.

Author Contributions

CW and LW contributed to the concept and designed the research study. ZW, JZ and CW performed the research. HS, ZW and WY provided help and advice on the experiments. LW and YD contributed to the analysis and interpretation of the data. All authors contributed to editorial changes in the manuscript. All authors read and approved the final manuscript. All authors have participated sufficiently in the work to take public responsibility for appropriate portions of the content and agreed to be accountable for all aspects of the work in ensuring that questions related to its accuracy or integrity.

Ethics Approval and Consent to Participate

This study was in line with the Declaration of Helsinki in the World Medical Association (WMA) and has been approved by the Medical Ethics Committee of the Third Affiliated Hospital of Qiqihar Medical College, with the number [2021] No. 101. Patients and their families who signed an informed consent after understanding the study contents.

Acknowledgment

Not applicable.

Funding

This research was funded by Heilongjiang Provincial Health Commission Scientific Research Project, grant number 20210909010194.

Conflict of Interest

The authors declare no conflict of interest.

References

[1] Dabli D, Frandon J, Belaouni A, Akessoul P, Addala T, Berny L, *et al*. Optimization of image quality and accuracy of low iodine concentration quantification as function of dose level and reconstruction algorithm for abdominal imaging using dual-source CT: A phantom study. Diagnostic and Interventional Imaging. 2022; 103: 31–40.

[2] Schuijf JD, Ko BS, Di Carli MF, Hislop-Jambrich J, Ihdayhid AR, Seneviratne SK, *et al*. Fractional flow reserve and myocardial perfusion by computed tomography: a guide to clinical application. European Heart Journal. Cardiovascular Imaging. 2018; 19: 127–135.

[3] Solomon J, Mileto A, Ramirez-Giraldo JC, Samei E. Diagnostic Performance of an Advanced Modeled Iterative Reconstruction Algorithm for Low-Contrast Detectability with a Third-Generation Dual-Source Multidetector CT Scanner: Potential for Radiation Dose Reduction in a Multireader Study. Radiology. 2015; 275: 735–745.

[4] Han BK, Grant KLR, Garberich R, Sedlmair M, Lindberg J, Lesser JR. Assessment of an iterative reconstruction algorithm (SAFIRE) on image quality in pediatric cardiac CT datasets. Journal of Cardiovascular Computed Tomography. 2012; 6: 200–204.

[5] Precht H, Kitslaar PH, Broersen A, Dijkstra J, Gerke O, Thygesen J, *et al*. Influence of Adaptive Statistical Iterative Reconstruction on coronary plaque analysis in coronary computed tomography angiography. Journal of Cardiovascular Computed Tomography. 2016; 10: 507–516.

[6] Zhong J, Xia Y, Chen Y, Li J, Lu W, Shi X, *et al*. Deep learning image reconstruction algorithm reduces image noise while alters radiomics features in dual-energy CT in comparison with conventional iterative reconstruction algorithms: a phantom study. European Radiology. 2023; 33: 812–824.

[7] Boudjelal A, Elmoataz A, Attallah B, Messali Z. A Novel Iterative MLEM Image Reconstruction Algorithm Based on Beltrami Filter: Application to ECT Images. Tomography. 2021; 7: 286–300.

[8] Ambrosanio M, Kosmas P, Pascazio V. A Multithreshold Iterative DBIM-Based Algorithm for the Imaging of Heterogeneous Breast Tissues. IEEE Transactions on Bio-Medical Engineering. 2019; 66: 509–520.

[9] Ghetti C, Ortenzia O, Serreli G. CT iterative reconstruction in image space: a phantom study. Physica Medica. 2012; 28: 161–165.

[10] Yasaka K, Katsura M, Akahane M, Sato J, Matsuda I, Ohtomo K. Model-based iterative reconstruction for reduction of radiation dose in abdominopelvic CT: comparison to adaptive statistical iterative reconstruction. SpringerPlus. 2013; 2: 209.

[11] Hou Y, Liu X, Xv S, Guo W, Guo Q. Comparisons of image quality and radiation dose between iterative reconstruction and filtered back projection reconstruction algorithms in 256-MDCT coronary angiography. AJR. American Journal of Roentgenology. 2012; 199: 588–594.

[12] Kang W. Personality Traits Predict Life Satisfaction in Coronary Heart Disease (CHD) Patients. Journal of Clinical Medicine. 2022; 11: 6312.

[13] Ciancarella P, Ciliberti P, Santangelo TP, Secchi F, Stagnaro N, Secinaro A. Noninvasive imaging of congenital cardiovascular defects. La Radiologia Medica. 2020; 125: 1167–1185.

[14] Patel VI, Roy SK, Budoff MJ. Coronary Computed Tomography Angiography (CCTA) vs Functional Imaging in the Evaluation of Stable Ischemic Heart Disease. The Journal of Invasive Cardiology. 2021; 33: E349–E354.

[15] Williams MC, Kwiecinski J, Doris M, McElhinney P, D'Souza MS, Cadet S, *et al*. Low-Attenuation Noncalcified Plaque on Coronary Computed Tomography Angiography Predicts Myocardial Infarction: Results From the Multicenter SCOT-HEART Trial (Scottish Computed Tomography of the HEART). Circulation. 2020; 141: 1452–1462.

[16] Pergola V, Continisio S, Mantovani F, Motta R, Mattesi G, Marrazzo G, *et al*. Spontaneous coronary artery dissection: the emerging role of coronary computed tomography. European Heart Journal. Cardiovascular Imaging. 2023; 24: 839–850.
[17] Prati F. Coronary computed tomography angiography in coronary heart disease: clinical applications and limitations. Giornale Italiano Di Cardiologia. 2019; 20: 409–416.
[18] Shu ZY, Cui SJ, Zhang YQ, Xu YY, Hung SC, Fu LP, *et al*. Predicting Chronic Myocardial Ischemia Using CCTA-Based Radiomics Machine Learning Nomogram. Journal of Nuclear Cardiology. 2022; 29: 262–274.
[19] Peper J, Becker LM, van den Berg H, Bor WL, Brouwer J, Nijenhuis VJ, *et al*. Diagnostic Performance of CCTA and CT-FFR for the Detection of CAD in TAVR Work-Up. JACC. Cardiovascular Interventions. 2022; 15: 1140–1149.
[20] Polidori T, De Santis D, Rucci C, Tremamunno G, Piccinni G, Pugliese L, *et al*. Radiomics applications in cardiac imaging: a comprehensive review. La Radiologia Medica. 2023; 128: 922–933.
[21] Choi AD. CT-FFR: Real-World Questions, and the New CAD Imaging Triple Aim. JACC. Cardiovascular Imaging. 2023; 16: 1066–1068.
[22] Nous FMA, Geisler T, Kruk MBP, Alkadhi H, Kitagawa K, Vliegenthart R, *et al*. Dynamic Myocardial Perfusion CT for the Detection of Hemodynamically Significant Coronary Artery Disease. JACC. Cardiovascular Imaging. 2022; 15: 75–87.
[23] Coenen A, Rossi A, Lubbers MM, Kurata A, Kono AK, Chelu RG, *et al*. Integrating CT Myocardial Perfusion and CT-FFR in the Work-Up of Coronary Artery Disease. JACC. Cardiovascular Imaging. 2017; 10: 760–770.
[24] World Medical Association. World Medical Association Declaration of Helsinki: ethical principles for medical research involving human subjects. JAMA. 2013; 310: 2191–2194.
[25] Nasir K, Cainzos-Achirica M. Role of coronary artery calcium score in the primary prevention of cardiovascular disease. British Medical Journal. 2021; 373: n776.
[26] Motoyama S, Ito H, Sarai M, Nagahara Y, Miyajima K, Matsumoto R, *et al*. Ultra-High-Resolution Computed Tomography Angiography for Assessment of Coronary Artery Stenosis. Circulation Journal. 2018; 82: 1844–1851.
[27] Antonopoulos AS, Angelopoulos A, Tsioufis K, Antoniades C, Tousoulis D. Cardiovascular risk stratification by coronary computed tomography angiography imaging: current state-of-the-art. European Journal of Preventive Cardiology. 2022; 29: 608–624.
[28] El Merhi F, Bou-Fakhredin R, El Ashkar B, Ghieh D, Ghosn Y, Saade C. State of the art of coronary computed tomography angiography. Radiography. 2020; 26: 174–182.
[29] Huang C, Yin C. A coronary artery CTA segmentation approach based on deep learning. Journal of X-Ray Science and Technology. 2022; 30: 245–259.
[30] Collet C, Onuma Y, Andreini D, Sonck J, Pompilio G, Mushtaq S, *et al*. Coronary computed tomography angiography for heart team decision-making in multivessel coronary artery disease. European Heart Journal. 2018; 39: 3689–3698.
[31] Gao W, Li X, Wang Y, Cai Y. Medical Image Segmentation Algorithm for Three-Dimensional Multimodal Using Deep Reinforcement Learning and Big Data Analytics. Frontiers in Public Health. 2022; 10: 879639.
[32] Gordic S, Desbiolles L, Sedlmair M, Manka R, Plass A, Schmidt B, *et al*. Optimizing radiation dose by using advanced modelled iterative reconstruction in high-pitch coronary CT angiography. European Radiology. 2016; 26: 459–468.
[33] Desai GS, Thabet A, Elias AYA, Sahani DV. Comparative assessment of three image reconstruction techniques for image quality and radiation dose in patients undergoing abdominopelvic multidetector CT examinations. The British Journal of Radiology. 2013; 86: 20120161.
[34] Nam SB, Jeong DW, Choo KS, Nam KJ, Hwang JY, Lee JW, *et al*. Image quality of CT angiography in young children with congenital heart disease: a comparison between the sinogram-affirmed iterative reconstruction (SAFIRE) and advanced modelled iterative reconstruction (ADMIRE) algorithms. Clinical Radiology. 2017; 72: 1060–1065.
[35] Örgel A, Bier G, Hennersdorf F, Richter H, Ernemann U, Hauser TK. Image Quality of CT Angiography of Supra-Aortic Arteries: Comparison Between Advanced Modelled Iterative Reconstruction (ADMIRE), Sinogram Affirmed Iterative Reconstruction (SAFIRE) and Filtered Back Projection (FBP) in One Patients' Group. Clinical Neuroradiology. 2020; 30: 101–107.
[36] Ayadi A, Sahtout W, Baledent O. A novel non-invasive method for estimating the local wave speed at a single site in the internal carotid artery. Biomedizinische Technik. 2020; 65: 557–566.
[37] Gould KL, Kirkeeide RL, Buchi M. Coronary flow reserve as a physiologic measure of stenosis severity. Journal of the American College of Cardiology. 1990; 15: 459–474.
[38] Javaid A, Ahmed AI, Han Y, Al Rifai M, Saad JM, Alfawara MS, *et al*. Incremental prognostic value of spect over CCTA. International Journal of Cardiology. 2022; 358: 120–127.
[39] Xia C, Vonder M, Pelgrim GJ, Rook M, Xie X, Alsurayhi A, *et al*. High-pitch dual-source CT for coronary artery calcium scoring: A head-to-head comparison of non-triggered chest versus triggered cardiac acquisition. Journal of Cardiovascular Computed Tomography. 2021; 15: 65–72.
[40] Ellmann S, Kammerer F, Allmendinger T, Hammon M, Janka R, Lell M, *et al*. Advanced Modeled Iterative Reconstruction (ADMIRE) Facilitates Radiation Dose Reduction in Abdominal CT. Academic Radiology. 2018; 25: 1277–1284.
[41] Tian C, Fei L, Zheng W, Xu Y, Zuo W, Lin CW. Deep learning on image denoising: An overview. Neural Networks. 2020; 131: 251–275.
[42] Nebelung H, Brauer T, Seppelt D, Hoffmann RT, Platzek I. Coronary computed tomography angiography (CCTA): effect of bolus-tracking ROI positioning on image quality. European Radiology. 2021; 31: 1110–1118.
[43] Winklehner A, Karlo C, Puippe G, Schmidt B, Flohr T, Goetti R, *et al*. Raw data-based iterative reconstruction in body CTA: evaluation of radiation dose saving potential. European Radiology. 2011; 21: 2521–2526.
[44] Xu C, Xu M, Yan J, Li YY, Yi Y, Guo YB, *et al*. The impact of deep learning reconstruction on image quality and coronary CT angiography-derived fractional flow reserve values. European Radiology. 2022; 32: 7918–7926.
[45] Tesche C, Gray HN. Machine Learning and Deep Neural Networks Applications in Coronary Flow Assessment: The Case of Computed Tomography Fractional Flow Reserve. Journal of Thoracic Imaging. 2020; 35: S66–S71.
[46] Tanigaki T, Emori H, Kawase Y, Kubo T, Omori H, Shiono Y, *et al*. QFR Versus FFR Derived From Computed Tomography for Functional Assessment of Coronary Artery Stenosis. JACC. Cardiovascular Interventions. 2019; 12: 2050–2059.
[47] Lee JM, Choi KH, Koo BK, Park J, Kim J, Hwang D, *et al*. Prognostic Implications of Plaque Characteristics and Stenosis Severity in Patients With Coronary Artery Disease. Journal of the American College of Cardiology. 2019; 73: 2413–2424.
[48] Li L, Hu X, Tao X, Shi X, Zhou W, Hu H, *et al*. Radiomic features of plaques derived from coronary CT angiography to identify hemodynamically significant coronary stenosis, using invasive FFR as the reference standard. European Journal of Radiology. 2021; 140: 109769.
[49] Cury RC, Leipsic J, Abbara S, Achenbach S, Berman D, Bittencourt M, *et al*. CAD-RADS™ 2.0 - 2022 Coronary Artery Disease-Reporting and Data System: An Expert Consensus Document of the Society of Cardiovascular Computed Tomog-

raphy (SCCT), the American College of Cardiology (ACC), the American College of Radiology (ACR), and the North America Society of Cardiovascular Imaging (NASCI). JACC. Cardiovascular Imaging. 2022; 15: 1974–2001.

[50] Min JK, Berman DS, Budoff MJ, Jaffer FA, Leipsic J, Leon MB, *et al*. Rationale and design of the DeFACTO (Determination of Fractional Flow Reserve by Anatomic Computed Tomographic AngiOgraphy) study. Journal of Cardiovascular Computed Tomography. 2011; 5: 301–309.

[51] Scholtz JE, Wichmann JL, Hüsers K, Albrecht MH, Beeres M, Bauer RW, *et al*. Third-generation dual-source CT of the neck using automated tube voltage adaptation in combination with advanced modeled iterative reconstruction: evaluation of image quality and radiation dose. European Radiology. 2016; 26: 2623–2631.

[52] von Knebel Doeberitz PL, De Cecco CN, Schoepf UJ, Duguay TM, Albrecht MH, van Assen M, *et al*. Coronary CT angiography-derived plaque quantification with artificial intelligence CT fractional flow reserve for the identification of lesion-specific ischemia. European Radiology. 2019; 29: 2378–2387.

[53] Zhuang B, Wang S, Zhao S, Lu M. Computed tomography angiography-derived fractional flow reserve (CT-FFR) for the detection of myocardial ischemia with invasive fractional flow reserve as reference: systematic review and meta-analysis. European Radiology. 2020; 30: 712–725.

[54] Khav N, Ihdayhid AR, Ko B. CT-Derived Fractional Flow Reserve (CT-FFR) in the Evaluation of Coronary Artery Disease. Heart, Lung & Circulation. 2020; 29: 1621–1632.

[55] Dey D, Lin A. Machine-Learning CT-FFR and Extensive Coronary Calcium: Overcoming the Achilles Heel of Coronary Computed Tomography Angiography. JACC. Cardiovascular Imaging. 2020; 13: 771–773.

[56] Park SK, Suh SH, Jang KS, Jang DK, Jo DY, Shin YS. Long-term clinical and angiographic outcome from angioplasty and stenting for intracranial stenosis. Acta Neurochirurgica. 2022; 164: 1627–1634.

[57] Leyvi G, Schechter CB, Sehgal S, Greenberg MA, Snyder M, Forest S, *et al*. Comparison of Index Hospitalization Costs Between Robotic CABG and Conventional CABG: Implications for Hybrid Coronary Revascularization. Journal of Cardiothoracic and Vascular Anesthesia. 2016; 30: 12–18.

[58] Tipograf Y, McLaren T, Savoie B, Kumar A, Levack MM. The role of coronary CTA and CT-fractional flow reserve evaluating coronary artery disease in transcatheter aortic valve replacement. Journal of Cardiac Surgery. 2022; 37: 4133–4137.

[59] Qiu L, Tan H, Cheng D, Shi H. The incremental clinical value of cardiac hybrid SPECT/CTA imaging in coronary artery disease. Nuclear Medicine Communications. 2018; 39: 469–478.

[60] Yang DH, Kang SJ, Koo HJ, Kweon J, Kang JW, Lim TH, *et al*. Incremental Value of Subtended Myocardial Mass for Identifying FFR-Verified Ischemia Using Quantitative CT Angiography: Comparison With Quantitative Coronary Angiography and CT-FFR. JACC. Cardiovascular Imaging. 2019; 12: 707–717.

[61] Manabe O, Naya M, Tamaki N. Feasibility of PET for the management of coronary artery disease: Comparison between CFR and FFR. Journal of Cardiology. 2017; 70: 135–140.

[62] Argacha JF, Decamp J, Vandeloo B, Babin D, Lochy S, Van den Bussche K, *et al*. Guiding Myocardial Revascularization by Algorithmic Interpretation of FFR Pullback Curves: A Proof of Concept Study. Frontiers in Cardiovascular Medicine. 2021; 8: 623841.

[63] Puymirat E, Cayla G, Simon T, Steg PG, Montalescot G, Durand-Zaleski I, *et al*. Multivessel PCI Guided by FFR or Angiography for Myocardial Infarction. New England Journal of Medicine. 2021; 385: 297–308.

[64] Neleman T, van Zandvoort LJC, Tovar Forero MN, Masdjedi K, Ligthart JMR, Witberg KT, *et al*. FFR-Guided PCI Optimization Directed by High-Definition IVUS Versus Standard of Care: The FFR REACT Trial. JACC. Cardiovascular Interventions. 2022; 15: 1595–1607.

[65] Chinnaiyan KM, Akasaka T, Amano T, Bax JJ, Blanke P, De Bruyne B, *et al*. Rationale, design and goals of the HeartFlow assessing diagnostic value of non-invasive FFR_*CT* in Coronary Care (ADVANCE) registry. Journal of Cardiovascular Computed Tomography. 2017; 11: 62–67.

[66] Beg F, Rehman H, Chamsi-Pasha MA, Nabi F, Chang SM, Mahmarian JJ, *et al*. Association Between FFR_*CT* and Instantaneous Wave-Free Ratio (iFR) of Intermediate Lesions on Coronary Computed Tomography Angiography. Cardiovascular Revascularization Medicine. 2021; 31: 57–60.

[67] Gajanan G, Samant S, Hovseth C, Chatzizisis YS. Case Report: Invasive and Non-invasive Hemodynamic Assessment of Coronary Artery Disease: Strengths and Weaknesses. Frontiers in Cardiovascular Medicine. 2022; 9: 885249.

[68] Chen YC, Zhou F, Wang YN, Zhang JY, Yu MM, Hou Y, *et al*. Optimal Measurement Sites of Coronary-Computed Tomography Angiography-derived Fractional Flow Reserve: The Insight From China CT-FFR Study. Journal of Thoracic Imaging. 2023; 38: 194–202.